*Proc. of the European Safety and Reliability Conference (ESREL 2026)*
*Edited by* José C. Matos, Paulo B. Lourenço, Michael Beer, Daniel Oliveira, Edoardo Patelli, Hélder S. Sousa, Rui A. Silva and Monica Santamaria

doi: 10.3850/ESREL2026061419_esrel26-p26206-cd

# A Petri Net Approach to Reliability and Degradation Modelling of a PEM Electrolyser

Salim Ubale, Rasa Remenyte-Prescott
*Resilience Engineering Research Group, University of Nottingham, Nottingham, UK.*
*E-mail:* salim.ubale@nottingham.ac.uk, r.remenyte-prescott@nottingham.ac.uk

David Grant, Alastair Stuart
*Advanced Materials Research Group, Faculty of Engineering, University of Nottingham, UK.*
*E-mail:* david.grant@nottingham.ac.uk, alastair.stuart@nottingham.ac.uk

Adam Hague
*ITM Power, UK, E-mail:* ahague@itm-power.com

Dynamic reliability modelling is crucial for complex, modern engineering systems such as proton exchange membrane (PEM) electrolysers, where multiple components interact and operating conditions may fluctuate significantly over time. In such systems, traditional static reliability assessment methods often necessitate oversimplifying assumptions and have limitations when it comes to accurately modelling phenomena, such as degradation, failures between individual cells within the stack, and their dependencies on variable environmental conditions. Addressing these challenges, this paper proposes a novel Petri Net-based approach to model the degradation and reliability characteristics of electrolysers. The Petri Net method is highly effective in representing dynamic behaviours, concurrent processes, and interdependencies, thereby offering a comprehensive framework for the evaluation of PEM electrolyser degradation and reliability. This approach accounts for concurrent degradation processes among the cells. Furthermore, the lifetime and operational performance of a PEM electrolyser are strongly influenced by a range of operating conditions, which include, temperature, pressure, and current density, all of which are incorporated into the model, given their significant impact on both cell degradation and overall system reliability. The developed model is computed using Monte Carlo simulation to determine cell-stack degradation, failure and reliability metrics over time. The findings aim to support and inform dynamic reliability assessment processes in the hydrogen industry.

*Keywords*: PEM Electrolyser, Petri Nets, Degradation, Reliability.

## 1. Introduction

Hydrogen energy systems, such as proton exchange membrane electrolysers (PEMEs), represent a viable approach for decarbonising sectors such as manufacturing and transportation. These systems must achieve high reliability (15–20 years), availability, and ease of maintenance while reducing costs. Reliability, availability, and maintainability (RAM) models can therefore be used to evaluate system performance. Recent announcements regarding hydrogen transmission infrastructure in the East Midlands area in the UK further emphasise the importance of robust reliability and asset management frameworks to ensure secure hydrogen supply at scale (EMCCA, 2026).

Traditional static reliability models typically assume independent component failures and binary operating states. However, PEM electrolyser systems operate under varying conditions where component degradation and failures evolve over time. Static techniques such as Fault Tree Analysis (FTA) and Reliability Block Diagrams (RBD) treat systems as memoryless, whereas dynamic approaches capture sequencing, timing, and state transitions between component conditions.

Dynamic reliability methods have been applied across a wide range of engineering domains, from high-risk industries such as nuclear and aerospace (Yan et al., 2023) to complex infrastructures including transportation networks and renewable energy systems (Le & Andrews, 2016). The choice of modelling technique depends on system characteristics. Highly redundant systems are often represented using dynamic fault trees or Markov models, while Petri Nets (PNs) are well suited to systems characterised by concurrency, continuous flows, and complex maintenance processes. Due to system complexity and uncertainty in reliability input data, reliability metrics are commonly evaluated using Monte Carlo simulation of the underlying model.

Petri Net-based reliability models have been applied across multiple engineering fields including nuclear safety analysis and railway infrastructure modelling (Yan et al., 2023). They have also been used to analyse degradation and reliability in fuel cells systems, where (Saleh et al., 2023)electrical, thermal, and fluid subsystems interact and degrade over time (Vasilyev et al., 2021; Whiteley et al., 2015a; Wieland et al., 2009a).

Despite these advances, only a few studies have addressed reliability and degradation modelling of PEM electrolysers under dynamic operating conditions. Therefore, this paper proposes a novel dynamic PN approach for reliability and degradation modelling of a PEME. The model captures concurrent degradation within the cell stack and incorporates key operating conditions, including operating power, water system condition, temperature, pressure, and current density, due to their significant influence on degradation behaviour and overall system reliability. Section 2 introduces the degradation parameters and operating conditions. Section 3 outlines the Petri Net concept. Section 4 presents the PEME PN model, followed by results in Section 5 and conclusions in Section 6.

## 2. Degradation parameter and operating conditions

### *2.1. Degradation rate*

The voltage degradation rate (D.R) quantifies the rate at which cell voltage increases over time under a constant load, hence measuring performance decline. It is frequently expressed in microvolts per hour (μV/h). Standard targets for modern PEME are <5 μV/hr. It is important to note that these values assume a linear voltage rise; however, degradation is often non-linear, as higher cell voltages accelerate several degradation mechanisms, including catalyst dissolution, membrane chemical degradation, and corrosion of porous transport layers and bipolar plates (Grigoriev et al., 2014a).

Using the US Department of Energy, 2022 status data for PEM electrolysers (Department of Energy, 2022), the average D.R is of 4.8 μV/h, and, at the beginning of life (BoL) a cell operates at about 1.9 V per cell at 2.0 A/cm² current density. The end of life (EoL) voltage is defined as a 10% rise in cell voltage at the same operating current. This corresponds to roughly 2.09 V per cell at 2.0 A/cm².

The lifetime can be estimated assuming a linear voltage rise over time. This equates to an approximate lifetime of ≈ 40,000 hours (about 4.5 years) of continuous operation. This is used to model the transitions between states for each PEME cell and is discussed in Section 4.

### *2.2. Operating conditions*

Degradation in a PEME has significant implications on the component's operation, performance and lifetime. These include membrane changes that can increase ionic resistivity or cause chemical oxidation, resulting in membrane thinning (Grigoriev et al., 2014b). Furthermore, degradation leads to reduced energy and coulombic efficiency, compromised gas purity, and heightened safety concerns with a risk of irreversible breakdown (Bessarabov & Millet, 2018). Understanding these consequences is crucial for optimising PEM electrolyser system operation, and maintenance.

PEME degradation mechanisms can be categorised into two groups. First, component-specific degradation mechanisms are associated with the main components of the electrolyser cell: the membrane, electrocatalyst layer, porous transport layer, and bipolar plate. They also arise from the complex interactions between individual components within the stack (Ubale et al., 2026).

Non-component degradation mechanisms result in from operating conditions, such as operating the cell/stack at very high current densities, contamination from inadequate water purification, and corrosion from upstream auxiliary components. The authors (Wallnöfer-Ogris et al., 2024) discuss component degradation mechanisms in their review study.

In addition to operating power and water system condition, the main operating conditions, such as temperature, pressure and current density, are considered in the proposed PN model.

PEM electrolyser degradation is strongly influenced by operating conditions, particularly power input, water management, pressure, current density, and temperature. Excessive or highly fluctuating power operation, which commonly arises from renewable energy coupling, induces thermal and mechanical stresses that accelerate membrane fatigue and catalyst corrosion (Endrődi et al., 2025). Degraded water conditions, including low flow rates or insufficient purity (≤1µS/cm), further exacerbate degradation. Ionic contaminants can poison the membrane and corrode catalysts, while inadequate water flow limits cooling and hydration, leading to membrane drying and localised overheating (Yoshimura et al., 2022) ; (Sun et al., 2015).

Although high-pressure operation (> 30 bar) does not dominate degradation mechanism, elevated pressure differentials increase mechanical stress on membranes and seals, and promote hydrogen and oxygen crossover, accelerating material degradation (Waite & Yazdani-Asrami, 2025). Similarly, operation beyond recommended current densities (> $2A/cm^2$) intensifies heat generation and gas bubble accumulation, creating localised hotspots that accelerate membrane and catalyst degradation (Khatib et al., 2019). Elevated temperatures (> 80° C) further accelerate chemical breakdown, membrane thinning, and corrosion, resulting in irreversible damage to the membrane electrode assembly (Maoulida et al., 2026a).

## 3. Petri Net definition

Petri Nets are a graphical and mathematical modelling tool developed for concurrent systems, and have been applied in reliability and availability analysis (Murata, 1989). Formal definitions and graphical notation of Petri Nets are standardised in ISO/IEC 15909-1 and EN 62551. A PN consists of *places* (p), which are states or conditions of a component or system. *Transitions* (t), which are linked by arcs to places, are events such as failures or repairs that may fire, and *tokens* that move through the net, enabling transitions. The places are respresented by circles and transitions are denoted by a rectangle. Tokens are represented by a dot in places, which represent that the place is marked and, therefore, move between places through the firing of transitions, enabling the dynamic evolution of system states.

The transitions have firing rates or probabilistic delays, which in this study are mainly associated with the times sampled form the exponential distribution or deterministic delays. Through token flow and transition firing, PNs can represent stochastic failure and repair process, as well as complex interactions such as concurrency, shared resources, and simultaneous events. In this study, places denote the status of a PEME component or operating condition, and transitions represent dynamic processes, such as degradation, failure, inspection, and maintenance.

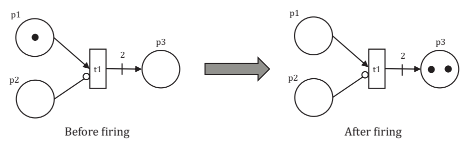


**Figure 1.** Petri Net example before and after firing

For example, in Figure 1, a simple PN is illustrated, where p1 and p2 represent the input places while p3 represents the output place, these are connected by the transition, t1. The place, p1 has a marking of 1 while p2 has a marking of 0. The place, p2 is connected to t1 via an inhibitor arc, as p2 is not marked with a token, the transition t1 is not inhibited and will fire as long as no token remains in place p2. The output arc has value of 2 which indicates its multiplicity, therefore 2 tokens are placed into p2 after t1 fires, and 1 token is removed from p1 (since the multiplicity is 1, commonly avoided from the diagram). The next section discusses the PEME model.

## 4. PEM Electrolyser model

### *4.1. Model description*

The hydrogen system PN model comprises four sub-models: degradation and failure sub-model, operating conditions sub-model, inspection, and maintenance sub-models. The four sub-models are interconnected within a single Petri Net framework. The operating conditions' sub-model influences the degradation and failure sub-model by modifying the firing rates of place-dependent degradation transitions when critical operating states are active. The degradation and failure sub-model determines the condition of individual cells and of the overall stack. The states of the stack are monitored by the inspection sub-model, which periodically reveals the true system condition. Based on the inspection outcome, the maintenance sub-model triggers replacement actions that restore system states and allow continued operation.

In this paper, two groups of PEME degradation mechanisms are explored. First, individual cell degradation contributes to the stack degradation and secondly, varied operational conditions such as operating the cell/stack in a critical power supply condition, very high current densities, high temperature, high pressure and critical water system condition, cell and stack degradation.

**Table 1.** Critical conditions and estimated degradation rates

| Operating condition | Voltage degradation rate (mV/h) | Average (mV/h) | Multiplier vs. baseline (4.8 µV/h) | Ref. |
|---|---|---|---|---|
| Critical PSU condition | 0.3–0.5 | 0.4 | 0.012 | (Suermann et al., 2019) |
| Critical water condition | 0.1–0.5 | 0.3 | 0.016 | (Rakousky et al., 2016) |
| High pressure condition | 0.1–0.2 | 0.15 | 0.0192 | Estimated |
| High current density condition | 0.3–0.5 | 0.4 | 0.012 | (Su et al., 2024) |
| High temperature condition | 0.2–0.4 | 0.3 | 0.016 | (Frensch et al., 2019) |

There is a shortage of quantitative data on how each operating condition affects the cell voltage. Therefore, the operating conditions and the estimated degradation rates and multipliers are presented in Table 1. Above-range conditions can increase degradation by one to two orders of magnitude. For instance, high current density (above $2A/cm^2$) or severe impurity levels may push degradation to ~0.5 mV/h (Su et al., 2024), over 100 times faster than the baseline, considerably shortening the stack's useful life. This is aggressive but credible under conditions of extreme stress or accelerated-test scenarios.

In addition, the literature (Maoulida et al., 2026b) has varying degradation rates reported under different conditions and stack sizes. Therefore, care is taken when estimating the degradation rates.

### *4.2. Degradation and failure sub-model*

This model comprises a stack of five cells. This study aims to examine the impact of changing operating conditions on each cell. The quantity of cells can be increased to a greater number of cells. As illustrated in Figure 2, each cell starts in its good place (p5, p9, p13, p17, p21). Three place-dependent (P.D) transitions per cell (e.g., t4–t6 for cell 1) independently fire tokens through minor-degraded, major-degraded, and failed places. The P.D transitions fire at a faster rate when any of the operating condition places are marked.

In parallel, the stack has four state places: good (p1), minor degraded (p2), major degraded (p3), and failed state (p4). The stack states are driven by counters p25–p27 that record how many cells at least are in the minor degraded, major degraded, or failed state.

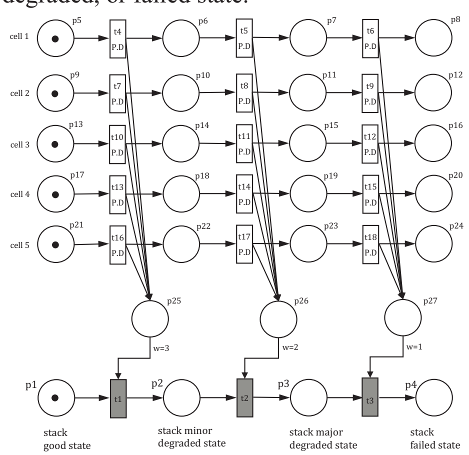


**Figure 2.** Cell-Stack degradation and failure sub-model

Weighted arcs (p25→t1 with a weight of 3, p26→t2 with a weight of 2, p27→t3 with a weight 1) advance the stack condition from p1→p2→p3→p4 when enough cells have degraded, i.e. for example, when 3 cells have degraded to the minor state, the stack moves to the minor degraded state (p2).

In the PN model, the cell degradation and failure transition times are determined based on the calculated lifetime in Eq (3), therefore, the time to failure (TTF) of each cell is ≈ 40,000 h. As illustrated in Figure 3, ($p_i$–$p_{iv}$) represent the cell places of cell 1–5, while the cell transitions ($t_a$, $t_b$, $t_c$), represent the transitions of the cells. It is assumed that the cell transitions are based on 20%, 50% and 100% of the TTF respectively.

### *4.3. Operating conditions sub-model*

In this model, each operating condition can be good or critical. A critical condition is an above-range deviation in an operating parameter that exceeds a specified upper control limit, either through sustained period or rapid transients, which can accelerate cell degradation. Below average limits are not considered in this model.

Five condition pairs represent these deviations or stressors, as illustrated in Figures 3, the PSU in good condition (p28) and critical condition (p29); the water system in good and critical condition (p30, p31); pressure normal (p32) and high (p33); current density normal (p34) and high (p35); and finally temperature normal, (p36), and high (p37).

The transitions (t19, t21, t23a, t24a, t25a) move tokens from normal to critical/high state; while the transitions (t20, t22, t23b, t24b, t25b) represent the recovery from critical/high state to good/normal condition. When any condition is in the critical/high state, i.e., any of the places (p29, p31, p33, p35, p37) are marked, the place-dependent transitions increase cell degradation rates, capturing load and environment induced acceleration.

In practice, the failure and recovery times for the operating conditions do not remain indefinitely abnormal; they have physical recovery paths. For example, overpressure events in PEM systems often dissipate when gas flows stabilise or when relief mechanisms operate. Therefore, recovery times can range from seconds to hours depending on system control. Due to data unavailability, the recovery times for each condition are estimated.

The transition parameters from normal to degraded or critical operating conditions (t19, t21, t23a, t24a, t25a) are assumed to follow exponential distributions because such failures are treated as memoryless random events. The parameters are presented in Table 2.

The exponential distribution is widely used to model the time between independent random occurrences such as component failures, abrupt pressure surges, or unanticipated current or temperature rises.

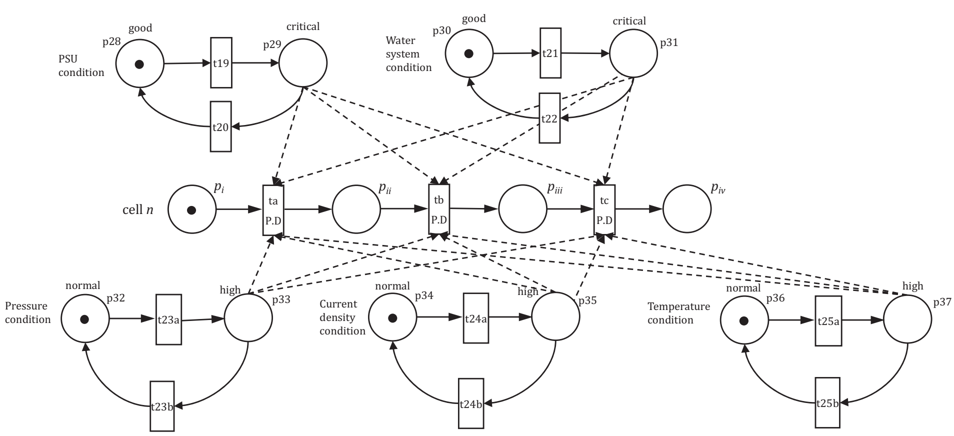


**Figure 3.** Operating conditions sub-model

**Table 2.** Operating conditions failure transitions

| Transition ID | Function | Transition parameter |
|---|---|---|
| t19 | PSU condition failure | exp ($1.0 \times 10^{-4}$) |
| t21 | Water condition failure | exp ($2.5 \times 10^{-4}$) |
| t23a | Pressure condition failure | exp ($2.0 \times 10^{-3}$) |
| t24a | Current density condition failure | exp ($2.5 \times 10^{-3}$) |
| t25a | Temperature condition failure | exp ($2.9 \times 10^{-3}$) |

The recovery transition parameters (t20, t22, t23b, t24b, t25b) follow a normal (Gaussian) distribution, reflecting processes such as physical stabilisation and control mechanisms. Recovery typically involves deterministic repair or stabilisation times (e.g., sensor response delays, control loop dynamics, or operator interventions).

### *4.4. Inspection and maintenance sub-model*

PEME inspection is planned every 3 months (2190 h).

As illustrated in Figure 4, a scheduled inspection event starts by t27 placing tokens into p44–p47, representing stack inspection while it is in the good, minor, major, failed states respectively, and marks p38 (system inspection).

For the true stack states (p40–p43), shown in Figure 5, the corresponding detection transition fires (p1 → t28 → p40, p2 → t29 → p45, p3→t30→p46, p4→t31→p43). For inspection branches in which the level of stack degradation

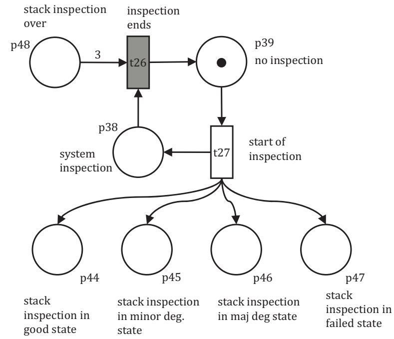


**Figure 4.** Inspection Petri Net sub-model

does not correspond to the detected level after inspection (revealed state), the transitions (t32–t35) fire from (p44–p47) to p48 (inspection is over). Once three tokens, which represent undetected conditions, are fired to p48, t26 fires and marks p39 (no inspection occurring).

The inhibitor arcs from (p1–p4) to (t32–t35) prevent from firing when there is a token is present in a stack state (p1–p4). Using the stack major degraded state as an example, if during inspection (p44–p47), the stack is in the major degraded state (p3), t30 will fire a token from p46 and p3 to p42 which corresponds to the revealed stack major degraded state.

The inhibitor arcs (p1–t32, p2–t33, p4–t35) allows (p44, p45, p47) to empty to p48 (stack inspection over) because the stack does not correspond to the level of degradation detected. Therefore, once there are 3 tokens in p48 due to (p44, p45, p47) emptying via (t32, t33, t35)

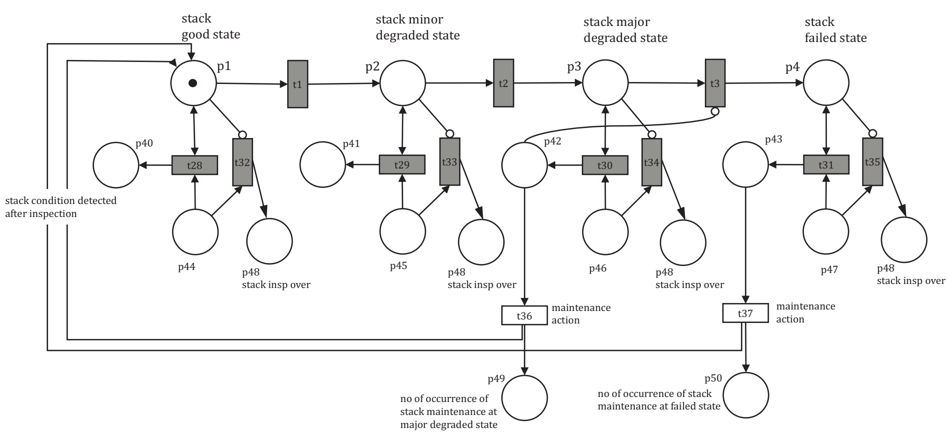


**Figure 5**. Stack maintenance Petri Net sub-model

respectively, t26 (end of inspection) fires a token to p39 (no inspection occurring).

## 5. Results and Discussion

The developed PN model was evaluated using Monte Carlo simulation with convergence achieved after 337 iterations. At each iteration, the simulation records the stack availability and updates the running estimate of the mean value. The variability of these estimates across iterations are quantified through the standard deviation. The simulation is confirmed to have converged once the variability falls below a tolerance of ±0.001. In addition, the degradation parameters used in the model are derived from values reported in the literature, allowing the simulated degradation behaviour and lifetime predictions to be compared with previously reported PEM electrolyser performance.

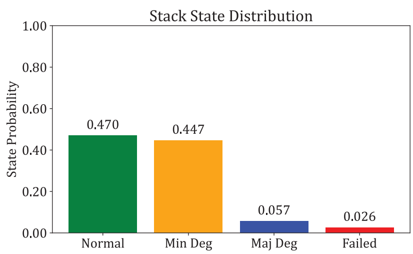


**Figure 6**. Stack state distribution

The results for one maintenance policy (replace major degraded and failed cells only) are shown in this section; however, many other maintenance policies can be modelled after the relevant modifications to the PN.

Figure 6 shows the probability of the stack being in the normal state is 0.470, whereas that of it being in the minor degraded state is 0.447. The probabilities of being in the major degraded or failed states are minimal.

In addition, the state distributions for each individual cell can also be obtained, as shown in Figure 7. The probability of each cell being in the normal state is around 0.53 and that of the minor degraded state is around 0.36. Since cell replacement occurs upon detection of the major degraded or failed stack condition, the probabilities of the cells remaining in good and minor degraded condition throughout the stack's lifetime are relatively high compared to the major degraded and failed states. The variation in individual cell probability values is due to randomness of the degradation process on each cell.

## 6. Conclusions

In this paper, the PN method is used to model PEME degradation, failure, inspection, and maintenance. This work extends previous studies by accounting for the contribution of individual cell degradation to stack degradation and by incorporating dynamic operating conditions, both of which strongly influence system reliability. The results highlight the importance of considering cell-level degradation, operating conditions, and maintenance policy selection when operating PEMEs.

The proposed model and its analysis can support asset management and operational

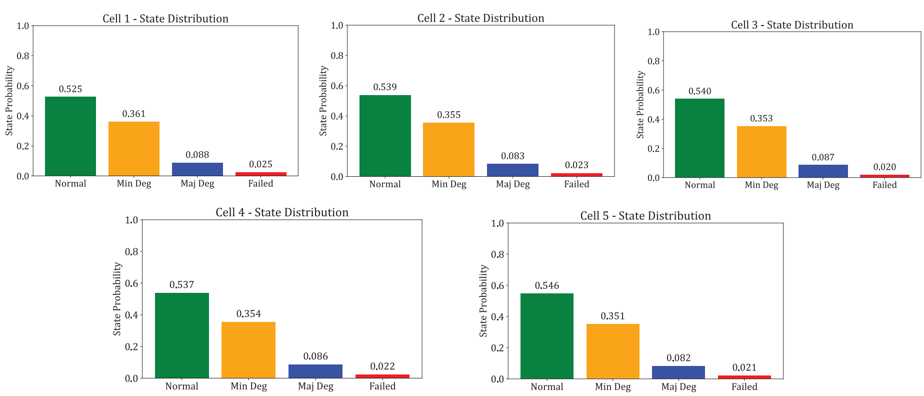


**Figure 7.** State distributions for each individual cells 1–5

decision-making, particularly in evaluating maintenance strategies, setting inspection intervals, and assessing the impact of operating condition thresholds on system availability. Operating condition parameter estimates influence simulation outcomes by determining the frequency of transitions into degraded or critical states. Overly conservative thresholds may lead to overestimation of degraded operation, resulting in reduced predicted availability and increased maintenance interventions.

Similarly, degradation multipliers applied under off-nominal operating conditions directly scale the rate of cell and stack deterioration. Higher multipliers shorten availability, while lower values delay degradation and extend operational lifetime.

Consequently, uncertainty in operating condition parameters can lead to variability in availability and maintenance predictions.

Future work will focus on uncertainty analysis, alternative maintenance policies, and explicit modelling of failure and repair processes in individual water system components. The system boundary may also be extended to include additional subsystems, such as hydrogen purification and compression, and to capture the effects of start-stop cycles known to accelerate specific electrolyser failure modes.

## Acknowledgement

The authors wish to express gratitude for the support received from the Sustainable Hydrogen Centre for Doctoral Training, the Engineering and Physical Sciences Research Council (EP/S023909/1), and ITM Power.

## References

Bessarabov, D., & Millet, P. (2018). Performance Degradation. In *PEM Water Electrolysis* (pp. 61–94). Elsevier. https://doi.org/10.1016/B978-0-08-102830-8.00003-5

Department of Energy. (2022). *Technical Targets for Proton Exchange Membrane Electrolysis*. https://www.energy.gov/eere/fuelcells/technical-targets-proton-exchange-membrane-electrolysis

EMCCA. (2026, January 22). *New 150km hydrogen pipeline to supply industry across Nottinghamshire and beyond - East Midlands Combined County Authority*. https://www.eastmidlands-cca.gov.uk/news/hydrogen-pipeline/

Endrődi, B., Trapp, C. A., Szén, I., Bakos, I., Lukovics, M., & Janáky, C. (2025). Challenges and Opportunities of the Dynamic Operation of PEM Water Electrolyzers. *Energies*, *18*(9), 2154. https://doi.org/10.3390/EN18092154/S1

Frensch, S. H., Fouda-Onana, F., Serre, G., Thoby, D., Araya, S. S., & Kær, S. K. (2019). Influence of the operation mode on PEM water electrolysis degradation. *International Journal of Hydrogen Energy*, *44*(57), 29889–29898. https://doi.org/10.1016/J.IJHYDENE.2019.09.169

Grigoriev, S. A., Dzhus, K. A., Bessarabov, D. G., & Millet, P. (2014a). Failure of PEM water electrolysis cells: Case study involving anode dissolution and membrane thinning. *Int J Hydrogen Energy*, *39*(35), 20440–20446. https://doi.org/10.1016/J.IJHYDENE.2014.05.043

Grigoriev, S. A., Dzhus, K. A., Bessarabov, D. G., & Millet, P. (2014b). Failure of PEM water electrolysis cells: Case study involving anode dissolution and membrane thinning. *International Journal of Hydrogen Energy*, *39*(35), 20440–20446. https://doi.org/10.1016/J.IJHYDENE.2014.05.043

Khatib, F. N., Wilberforce, T., Ijaodola, O., Ogungbemi, E., El-Hassan, Z., Durrant, A., Thompson, J., & Olabi, A. G. (2019). Material degradation of components in polymer electrolyte membrane (PEM) electrolytic cell and mitigation mechanisms: A review. *Renewable and Sustainable Energy Reviews*, *111*, 1–14. https://doi.org/10.1016/J.RSER.2019.05.007

Le, B., & Andrews, J. (2016). Modelling wind turbine degradation and maintenance. *Wind Energy*, *19*(4), 571–591. https://doi.org/10.1002/WE.1851

Maoulida, F., Guilbert, D., Camara, M. B., & Dakyo, B. (2026a). Dynamic electrical degradation of PEM electrolyzers under renewable energy Intermittency: Mechanisms, diagnostics, and mitigation strategies – A comprehensive review. *Renewable and Sustainable Energy Reviews*, *225*, 116170. https://doi.org/10.1016/J.RSER.2025.116170

Maoulida, F., Guilbert, D., Camara, M. B., & Dakyo, B. (2026b). Dynamic electrical degradation of PEM electrolyzers under renewable energy Intermittency: Mechanisms, diagnostics, and mitigation strategies – A comprehensive review. *Renewable and Sustainable Energy Reviews*, *225*, 116170. https://doi.org/10.1016/J.RSER.2025.116170

Murata, T. (1989). Petri Nets: Properties, Analysis and Applications. *Proceedings of the IEEE*, *77*(4), 541–580. https://doi.org/10.1109/5.24143

Rakousky, C., Reimer, U., Wippermann, K., Carmo, M., Lueke, W., & Stolten, D. (2016). An analysis of degradation phenomena in polymer electrolyte membrane water electrolysis. *J Power Sources*, *326*, 120–128. https://doi.org/10.1016/j.jpowsour.2016.06.082

Saleh, A., Prescott, D., Remenyte, R., & Chiachio, M. (2023). An optimized asset management petri net model for railway sections. *Materials Research Proceedings*, *27*, 285–291. https://doi.org/10.21741/9781644902455-37

Su, Z., Liu, J., Li, P., & Liang, C. (2024). Study of the Durability of Membrane Electrode Assemblies in Various Accelerated Stress Tests for Proton-Exchange Membrane Water Electrolysis. *Materials*, *17*(6), 1331. https://doi.org/10.3390/MA17061331/S1

Suermann, M., Bensmann, B., & Hanke-Rauschenbach, R. (2019). Degradation of Proton Exchange Membrane (PEM) Water Electrolysis Cells: Looking Beyond the Cell Voltage Increase. *J Electrochem Soc*, *166*(10), F645–F652. https://doi.org/10.1149/2.1451910JES/XML

Sun, S., Xiao, Y., Liang, D., Shao, Z., Yu, H., Hou, M., & Yi, B. (2015). Behaviors of a proton exchange membrane electrolyzer under water starvation. *RSC Advances*, *5*(19), 14506–14513. https://doi.org/10.1039/C4RA14104K

Ubale, S., Remenyte-Prescott, R., Grant, D. M., Stuart, A., & Hague, A. (2026). Failure and reliability analysis of PEM electrolyser balance of plant. *Renewable Energy*, *256*, 124029. https://doi.org/10.1016/J.RENENE.2025.124029

Vasilyev, A., Andrews, J., Dunnett, S. J., & Jackson, L. M. (2021). Dynamic Reliability Assessment of PEM Fuel Cell Systems. *Reliab Eng Syst Saf*, *210*, 107539. https://doi.org/10.1016/j.ress.2021.107539

Waite, T., & Yazdani-Asrami, M. (2025). Degradation modeling of polymer electrolyte membrane water electrolyzers for hydrogen production: motivation, status, and strategies. *Journal of Physics: Energy*, *7*(4), 042002. https://doi.org/10.1088/2515-7655/ADE9F0

Wallnöfer-Ogris, E., Grimmer, I., Ranz, M., Höglinger, M., Kartusch, S., Rauh, J., Macherhammer, M. G., Grabner, B., & Trattner, A. (2024). A review on understanding and identifying degradation mechanisms in PEM water electrolysis cells: Insights for stack application, development, and research. *International Journal of Hydrogen Energy*, *65*, 381–397. https://doi.org/10.1016/J.IJHYDENE.2024.04.017

Whiteley, M., Fly, A., Leigh, J., Dunnett, S., & Jackson, L. (2015). Advanced reliability analysis of Polymer Electrolyte Membrane Fuel Cells using Petri-Net analysis and fuel cell modelling techniques. *International Journal of Hydrogen Energy*, *40*(35), 11550–11558. https://doi.org/10.1016/J.IJHYDENE.2015.01.154

Wieland, C., Schmid, O., Meiler, M., Wachtel, A., & Linsler, D. (2009). Reliability computing of polymer-electrolyte-membrane fuel cell stacks through Petri nets. *Journal of Power Sources*, *190*(1), 34–39. https://doi.org/10.1016/J.JPOWSOUR.2008.10.010

Yan, R., Dunnett, S., & Andrews, J. (2023). A Petri net model-based resilience analysis of nuclear power plants under the threat of natural hazards. *Reliability Engineering & System Safety*, *230*, 108979. https://doi.org/10.1016/J.RESS.2022.108979

Yoshimura, R., Wai, S. H., Ota, Y., Nishioka, K., & Suzuki, Y. (2022). Effects of Artificial River Water on PEM Water Electrolysis Performance. *Catalysts 2022, Vol. 12, Page 934*, *12*(9), 934. https://doi.org/10.3390/CATAL12090934